

See discussions, stats, and author profiles for this publication at: <https://www.researchgate.net/publication/262055310>

Structure-based 3D-QSAR studies on quinazoline derivatives as platelets-derived growth factor (PDGFR) inhibitors

ARTICLE *in* MEDICINAL CHEMISTRY RESEARCH · SEPTEMBER 2014

Impact Factor: 1.4 · DOI: 10.1007/s00044-014-0946-8

READS

74

4 AUTHORS:



Zaheer Ulhaq

University of Karachi

101 PUBLICATIONS 941 CITATIONS

SEE PROFILE



Syed Kashif

University of Karachi

2 PUBLICATIONS 0 CITATIONS

SEE PROFILE



Naveed Khan

Chinese Academy of Sciences PICB, Shangh...

1 PUBLICATION 0 CITATIONS

SEE PROFILE



Uzma Mahmood

University of Karachi

10 PUBLICATIONS 33 CITATIONS

SEE PROFILE

Structure-based 3D-QSAR studies on quinazoline derivatives as platelets-derived growth factor (PDGFR) inhibitors

Zaheer Ul-Haq · Syed Kashif Zafar ·
Naveed Khan · Uzma Mahmood

Received: 28 August 2013 / Accepted: 7 February 2014
© Springer Science+Business Media New York 2014

Abstract Platelet-derived growth factor (PDGF) is one of the various growth factors, which involves in regulation of cell growth and division. In this work, 3D-quantitative structure–activity relationship studies of 75 quinazolines derivative as PDGFR’s inhibitor were performed. Based on the cognate ligand (PBD code: 3MJG 2.3 Å), numerous alignment methods were used to obtain reliable comparative molecular field analysis (CoMFA) and comparative molecular similarity indices (CoMSIA) models. Docked pose of the most active compound followed by database alignment led to derived best CoMFA model ($q^2 = 0.531$, $r_{ncv}^2 = 0.913$). With the same alignment, a statistically reliable CoMSIA model with all the five fields was also derived ($q^2 = 0.525$, $r_{ncv}^2 = 0.889$). A test set was used to validate both the models, which gave satisfactory predictive (r_{pred}^2) values of 0.77 and 0.79, respectively. Contour maps of CoMFA and CoMSIA revealed the effect of important structural features on biological activity within the binding pocket and explained its interactions with ligand.

Keywords Platelet-derived growth factor (PDGF) · 3D-quantitative structure–activity relationship studies (3D-QSAR) · CoMFA · CoMSIA · Docking studies · GOLD

Introduction

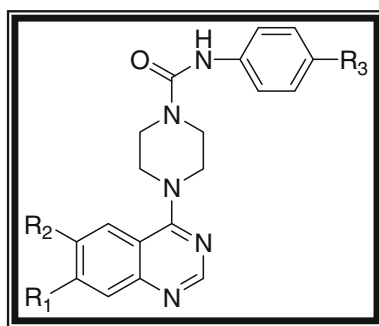
Receptor tyrosine kinase (RTK’s) constitutes a large family of growth factors, all of which contain an integral protein tyrosine kinase (PTK) (Zhong *et al.*, 2004; Shim *et al.*, 2010; Kurup *et al.*, 2001). The structure consists of three parts, a ligand binding region on the cell membrane, a membrane spanning region, and an intracellular cytoplasmic domain for the binding of PTK (Guha and Jurs, 2004). Upon ligand binding to these receptors, a growth signal is generated that initiates cascade of events followed by phosphorylation of tyrosine residues (Kurup *et al.*, 2001). Growth factors like EGF, platelet-derived growth factor (PDGF), FGF, VEGF, and IGF-I belong to RTKs are involved in regulating cellular growth and development (Kurup *et al.*, 2001; Guha and Jurs, 2004; Pandey *et al.*, 2002). Genetic mutations in RTK’s caused oncogene disorders, either by continuous activation of the receptors in the absence of ligand or by overexpression of these receptors due to abnormal, uncontrolled proliferative activity of the growth factors (Kurup *et al.*, 2001). The main concern of our study is platelet-derived growth factor receptor (PDGFR) inhibitors, one of the most widely studied inhibitors of tyrosine kinase. Its family includes α -PDGFR, β -PDGFR, colony stimulating factor-1 (CSF-1), FLT-3, and C-KIT (Pandey *et al.*, 2002). PDGFR inhibitors are exclusively involved in signal transduction mechanisms rather than in interfering with DNA synthesis. Because of this function, our research will be focused on improving the selectivity for PDGFR inhibitors, a major problem with conventional

Z. Ul-Haq (✉) · S. K. Zafar · N. Khan
Dr. Panjwani Center for Molecular Medicine and Drug Research,
International Center for Chemical and Biological Sciences,
University of Karachi, Karachi 75270, Pakistan
e-mail: zaheer.qasmi@iccs.edu

Z. Ul-Haq
Heidelberg Institute for Theoretical Studies, HITS gGmbH,
Schloss-Wolfsbrunnengasse 35, 69118 Heidelberg, Germany

U. Mahmood
Department of Chemistry, University of Karachi, Karachi 75270,
Pakistan

U. Mahmood
Aligarh Institute of Technology, Block-5, Gulshan-e-Iqbal,
University Road, Karachi 75300, Pakistan

Table 1 Molecular structures of 4-[4-(N-substituted thiocarbamoyl)-1-piperazinyl]-6,7-dimethoxyquinazolines and their derivatives with experimental pIC₅₀ values

Compounds	R ₁	R ₂	R ₃	pIC ₅₀
1			t-Bu	8.85
2			CN	6.80
3				8.80
4				9.40
5				9.40
6				9.00
7				7.70
8				8.00
9				7.92

Table 1 continued

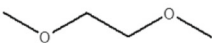
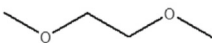
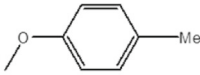
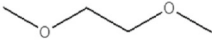
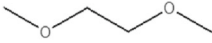
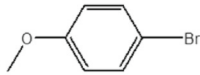
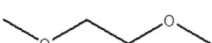
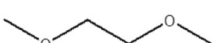
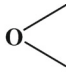
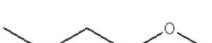
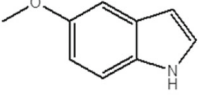
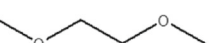
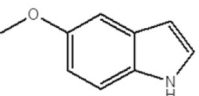
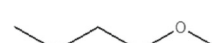
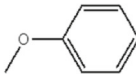
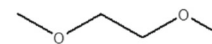
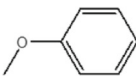
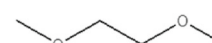
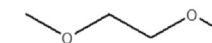
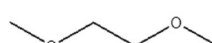
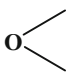
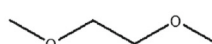
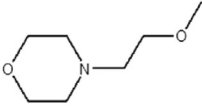
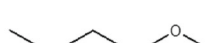
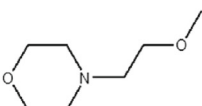
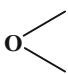
Compounds	R ₁	R ₂	R ₃	pIC ₅₀
10				8.59
11				8.62
12				7.30
13		OMe		8.05
14		H		8.70
15		OMe		7.40
16		H		7.40
17		OMe	CN	5.89
18		H	CN	5.90
19		OMe		6.38
20			CN	5.96
21				5.30

Table 1 continued

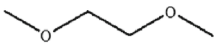
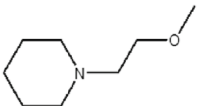
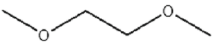
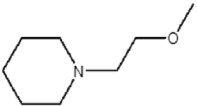
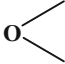
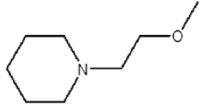
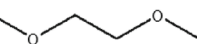
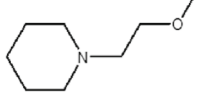
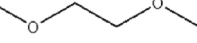
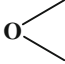
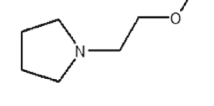
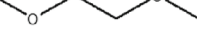
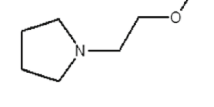
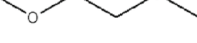
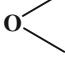
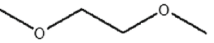
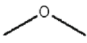
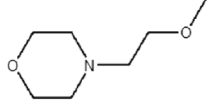
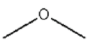
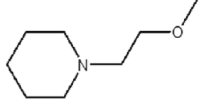
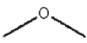
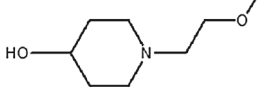
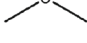
Compounds	R ₁	R ₂	R ₃	pIC ₅₀
22			CN	6.30
23				6.70
24			CN	7.10
25				7.00
26			CN	6.77
27				6.84
28			CN	5.89
29			CN	5.85
30			CN	6.37
31			CN	5.21

Table 1 continued

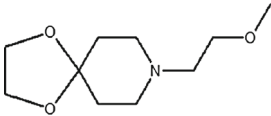
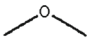
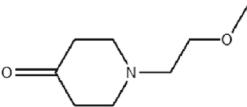
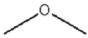
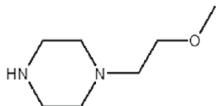
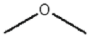
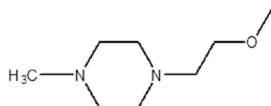
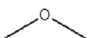
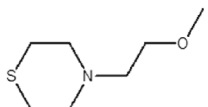
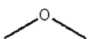
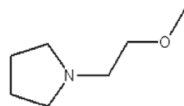
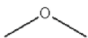
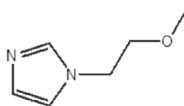
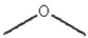
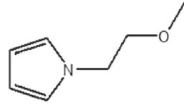
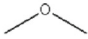
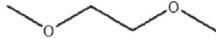
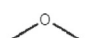
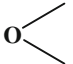
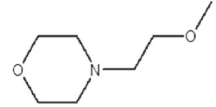
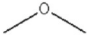
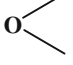
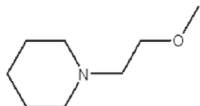
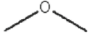
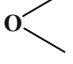
Compounds	R ₁	R ₂	R ₃	pIC ₅₀
32			CN	6.47
33			CN	5.86
34			CN	5.19
35			CN	6.12
36			CN	6.35
37			CN	6.82
38			CN	5.09
39			CN	6.15
40				6.38
41				6.70
42				5.90

Table 1 continued

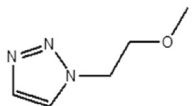
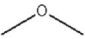
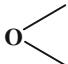
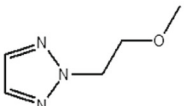
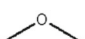
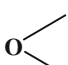
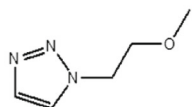
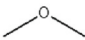
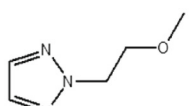
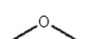
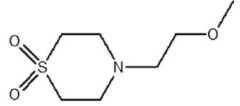
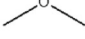
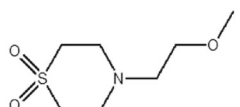
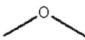
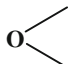
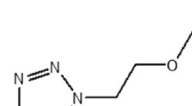
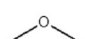
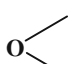
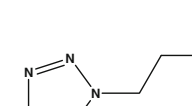
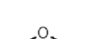
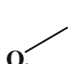
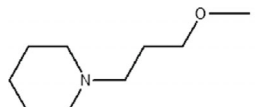
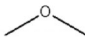
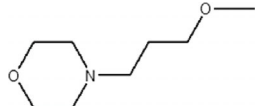
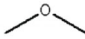
Compounds	R ₁	R ₂	R ₃	pIC ₅₀
43				6.47
44				6.28
45			CN	5.65
46			CN	5.92
47			CN	5.67
48				6.31
49				6.29
50				6.67
51			CN	7.28
52			CN	6.84

Table 1 continued

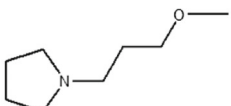
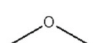
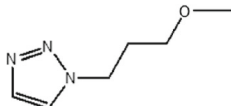
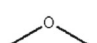
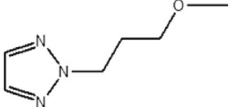
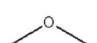
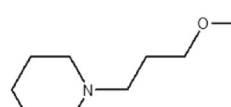
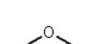
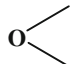
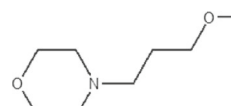
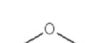
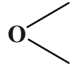
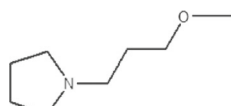
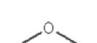
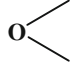
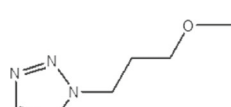

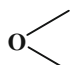
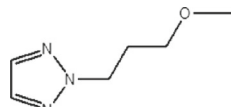
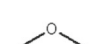
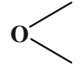
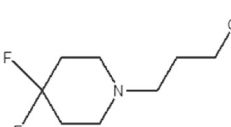

Compounds	R ₁	R ₂	R ₃	pIC ₅₀
53			CN	6.75
54			CN	5.55
55			CN	6.03
56				7.59
57				7.70
58				7.11
59				5.84
60				6.10
61			CN	6.96

Table 1 continued

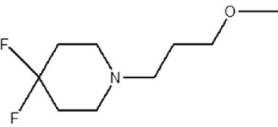
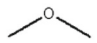
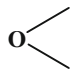
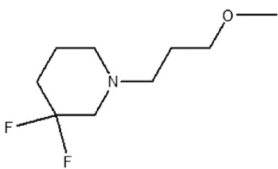
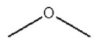
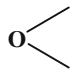
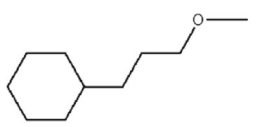
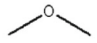
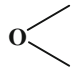
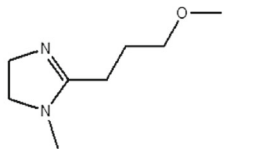
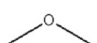
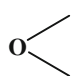
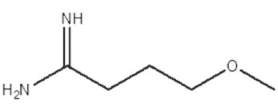
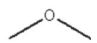
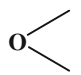
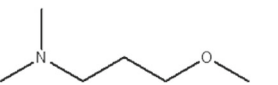
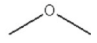
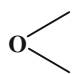
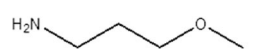
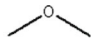
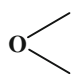
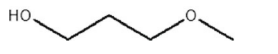
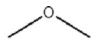
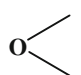
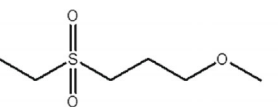
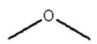
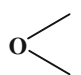
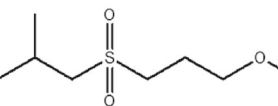
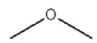
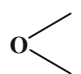
Compounds	R ₁	R ₂	R ₃	pIC ₅₀
62				7.40
63				7.54
64				6.09
65				4.91
66				6.06
67				7.12
68				5.51
69				5.25
70				6.39
71				7.44

Table 1 continued

Compounds	R ₁	R ₂	R ₃	pIC ₅₀
72				7.06
73				6.95
74				7.30
75				6.25

chemotherapeutic agents (Guha and Jurs, 2004). Several studies have reported PDGFR inhibition activity with different compounds including 3-arylquinolines, 3-arylquinolines, phenylaminopyrimidines, pyrazoles, and phenylbenzimidazoles (Guha and Jurs, 2004). PDGFR inhibitory activity may also decrease the interstitial fluid pressure within solid tumors that is responsible for enhancing drug delivery. Because ATP binding and phosphorylation of tyrosine residues confer the PDGFR inhibitory activity, an analog of PDGFR, 4-[4-(N-substituted thiocarbamoyl)-1-piperazinyl]-6,7-dimethoxyquinazoline, is considered as a potent inhibitor (Pandey *et al.*, 2002). A 2D-QSAR study has already been reported on the dataset under consideration for our study (Guha and Jurs, 2004). In the current study, 3D-QSAR studies were performed on 75 human plasma piperazinylquinazolines inhibitors of TRKs by using a structure-based molecular docking protocol followed by comparative molecular field analysis (CoMFA) and comparative molecular similarity indices (CoMSIA) technique. These computational techniques are widely used to find associations between chemical structures and their biological activities in space where activity may influence by interactive fields and useful to predict new novel compounds against PDGFR.

Materials and methods

A set of 75 compounds with their IC₅₀ (μM) values against PDGFR were retrieved from the literature (Pandey *et al.*,

2002). Extensive molecular docking studies were carried out to determine the binding mode of piperazinylquinazolines compounds within the PDGFR active site. The conformations obtained by molecular docking methodology are utilized in molecular alignment. Subsequently, database alignment was used to align all compounds on the dock pose of active compound.

The structures of entire sets of 4-[4-(N-substituted thiocarbamoyl)-1-piperazinyl]-6,7-dimethoxyquinazolines were retrieved in mol format from the freely available cheminformatics database. SYBYL7.3 is used for atom type corrections, energy minimizations, and charge protocol. Gasteiger and Marsili (1980) atomic charges were assigned on the whole dataset before performing energy minimization using Tripos molecular mechanics force field (Clark *et al.*, 1989) with Powell's conjugate gradient algorithm until 0.05 kcal/mol Å value of convergence criterion was reached (Zhang and Zhong, 2010; Seymour *et al.*, 1991). The dataset of 75 compounds was distributed into training and test sets (Tables 1, 2). The selection criteria for both the datasets are based on structurally diverse molecules with a wide range of activities were included with a ratio of 4:1. For the construction of CoMFA and CoMSIA models, 61 compounds were taken in the training set and the remaining 14 compounds were kept in the test set.

The only experimentally resolved crystal structure of PDGFR is present in a dimer form in the RCSB Protein Data Bank (PDB code: 3MJG 2.3 Å resolution) (Shim

Table 2 Actual versus predicted inhibitory activities of 4-[4-(N-substituted thiocarbamoyl)-1-piperazinyl]-6,7-dimethoxyquinazolines derivatives with residual of training and test set

Compounds	Actual (pIC ₅₀)	CoMFA		CoMSIA	
		Predicted (pIC ₅₀)	Residual	Predicted (pIC ₅₀)	Residual
1	8.85	8.53	0.32	8.201	0.65
2	6.80	7.14	−0.34	7.179	−0.38
3 ^a	8.80	8.811	−0.01	8.811	−0.01
4	9.40	9.86	−0.46	9.679	−0.28
5	9.40	9.58	−0.17	9.368	0.03
6	9.00	8.81	0.2	8.707	0.29
7	7.70	7.69	0.01	7.737	−0.04
8 ^a	8.00	7.95	0.05	7.63	0.37
9	7.92	8.04	−0.12	8.166	−0.25
10	8.59	8.29	0.3	8.436	0.15
11 ^a	8.62	7.54	1.08	7.617	1
12	7.30	7.06	0.24	7.164	0.14
13	8.05	8.09	−0.04	8.032	0.02
14	8.70	8.87	−0.17	8.97	−0.27
15	7.40	6.84	0.56	6.898	0.5
16 ^a	7.40	6.89	0.51	7.009	0.39
17	5.89	6.08	−0.19	6.219	−0.33
18	5.90	6.52	−0.62	6.455	−0.55
19	6.38	6.26	0.12	6.65	−0.27
20	5.96	5.94	0.02	6.189	−0.23
21	5.30	5.87	−0.57	5.979	−0.68
22	6.30	6.16	0.14	6.251	0.05
23	6.70	6.63	0.07	6.645	0.06
24	7.10	6.85	0.25	6.823	0.28
25	7.00	7.11	−0.11	7.196	−0.2
26	6.77	6.92	−0.15	6.947	−0.18
27	6.84	7.12	−0.28	7.246	−0.41
28	5.89	6.03	−0.14	6.22	−0.33
29 ^a	5.85	6.09	−0.24	5.676	0.17
30 ^a	6.37	5.88	0.49	5.933	0.44
31	5.21	5.76	−0.55	5.615	−0.41
32	6.47	6.11	0.36	6.426	0.04
33	5.86	5.75	0.11	5.706	0.15
34 ^a	5.19	6.03	−0.84	5.953	−0.76
35	6.12	6.12	0	6.307	−0.19
36	6.35	6.03	0.32	6.006	0.34
37	6.82	6.27	0.55	6.146	0.67
38	5.09	5.35	−0.25	5.676	−0.59
39	6.15	5.84	0.31	5.57	0.58
40	6.38	6.24	0.14	6.656	−0.28
41	6.70	6.28	0.42	6.058	0.64
42	5.90	6.03	−0.13	6.302	−0.4
43	6.47	6.41	0.06	6.303	0.17
44	6.28	6.40	−0.12	6.257	0.02
45	5.65	6.14	−0.49	5.851	−0.2

Table 2 continued

Compounds	Actual (pIC ₅₀)	CoMFA		CoMSIA	
		Predicted (pIC ₅₀)	Residual	Predicted (pIC ₅₀)	Residual
46	5.92	6.04	−0.12	5.67	0.25
47	5.67	5.80	−0.13	5.547	0.12
48	6.31	6.12	0.19	5.929	0.38
49	6.29	6.06	0.23	6.021	0.27
50 ^a	6.67	6.27	0.4	6.359	0.31
51 ^a	7.28	7.06	0.22	6.951	0.33
52	6.84	6.92	−0.08	6.957	−0.12
53	6.75	6.97	−0.22	6.884	−0.13
54 ^a	5.55	5.43	0.12	5.666	−0.12
55 ^a	6.03	5.85	0.18	5.774	0.26
56	7.59	7.41	0.18	7.349	0.24
57 ^a	7.70	7.26	0.44	7.404	0.3
58	7.11	7.04	0.07	7.191	−0.08
59	5.84	5.59	0.25	5.889	−0.05
60	6.10	5.98	0.12	6.16	−0.06
61 ^a	6.96	6.93	0.03	6.744	0.22
62	7.40	7.38	0.02	7.185	0.22
63	7.54	7.60	−0.06	7.241	0.3
64	6.09	6.12	−0.03	6.292	−0.2
65	4.91	7.16	−2.25	7.139	−2.23
66	6.06	6.29	−0.23	5.654	0.41
67	7.12	6.34	0.78	6.579	0.54
68	5.51	5.98	−0.47	5.421	0.09
69 ^a	5.25	5.86	−0.61	5.85	−0.6
70	6.39	6.57	−0.18	6.66	−0.27
71	7.44	7.10	0.34	7.095	0.34
72	7.06	6.96	0.1	6.849	0.21
73	6.95	6.64	0.31	6.699	0.25
74	7.30	7.13	0.18	7.169	0.13
75	6.25	6.54	−0.29	6.846	−0.6

^a Test set compounds

et al., 2010). Monomer form of PDGFR was utilized for docking experiments with cystine knot beta-sheet structure. Docked conformations produced unsatisfactory results for our 3D-QSAR studies. However, in an alternate approach, top ranked docked conformation for the biologically most active inhibitor (compound **5**) was selected as a template to align rest of the compounds. Five different points were selected from the core group of compound **5** in Fig. 1. For database alignment (Fig. 2), a sp³ hybridized carbon atom with net negative charge as the probe atom is used with truncated energy set as 30 kcal/mol (Gupta *et al.*, 2009; Geldenhuys and Nakamura, 2010; Sethi *et al.*, 2010; Du-Cuny *et al.*, 2009). Calculations were carried out using Lennard–Jones 6–12 potential and Coulombic potential (Ul-Haq *et al.*, 2009) functions, contained by Tripos force

field (Klebe *et al.*, 1994) with a distance-dependent dielectric constant ($1/r$). The CoMFA fields generated automatically and scaled by the CoMFA-STD method.

CoMSIA (Geladi *et al.*, 1998) is an advance method of CoMFA with three additional fields (hydrogen bond donor, hydrogen bond acceptor, and hydrophobic). It is used to avoid some inherent deficiencies arising from the steric and electrostatic (Lennard–Jones and Coulomb potentials) fields of CoMFA descriptors. Distance-dependent Gaussian-type functional form is introduced in CoMSIA. To generate steric field energies, a sp^3 hybridized carbon atom served as probe atom and a charge of +1.0 is used for electrostatic field energies. For other descriptors in CoMSIA calculations, a sp^3 hybridized carbon atom is also used as a probe atom with a +1 hydrophobicity, +1 H-bond donor, and +1 H-bond acceptor properties (Qin *et al.*, 2010). The default value of attenuation factor 0.3 was used (Clark *et al.*, 1989).

Partial least squares (PLS) method was used to establish a correlation between physiochemical property (dependant variable) and molecular fields (independent variables) for training set. Leave one out (LOO) method (Cramer *et al.*, 1988) was used for the evaluation of both CoMFA and CoMSIA models. Optimum number of components (ONC) was estimated by the conjunction of PLS (Roques *et al.*, 1993) with cross-validation which is further helpful to generate CoMFA and CoMSIA model with non-cross-validation method. This value was used to assess prediction ability for both generated models. Following equation is used to calculate the r^2_{pred} for the test set

$$r^2_{pred} = 1 - \frac{PRESS}{SD}.$$

The graphical interpretation of CoMFA/CoMSIA results was performed by “STdev*Coeff” field type.

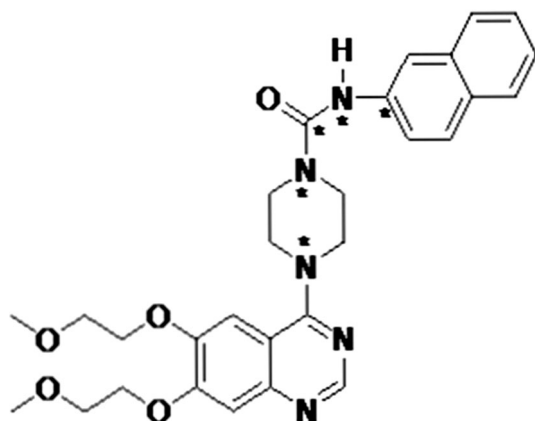


Fig. 1 Template structure used for the database alignment and selected atoms are indicated by asterisk

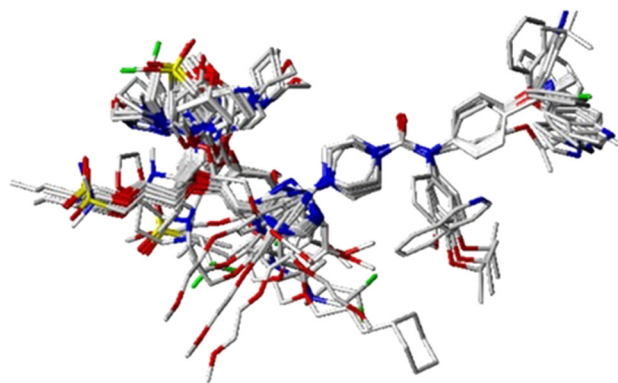


Fig. 2 Database alignment of whole dataset containing 75 different analogs of 4-[4-(N-substituted thiocarbonyl)-1-piperazinyl]-6,7-dimethoxyquinazolines

Results and discussion

Statistical parameters for CoMFA and CoMSIA models of PDGFR inhibitors were generated using 3D-QSAR (Table 3). The CoMFA statistical results gave a cross-validated correlation (q^2) of 0.531 with 5 ONC. The non-cross-validated correlation coefficient (r^2) was 0.913 with a low standard error estimate (SEE) of 0.313 and a predictive correlation coefficient (r^2_{pred}) of 0.77. Steric and electrostatic fields contributed 51.7 and 48.3 %, respectively. Using all five descriptors, the CoMSIA model gave a cross-validated correlation coefficient value of 0.52 with an ONC 4 and a non-cross-validated correlation coefficient value of 0.889. CoMSIA model was validated by the test set with a (r^2_{pred}) value of 0.79. The actual and predicted pIC_{50} values and their residuals for training and test sets are shown in Table 2. The actual and predicted activities (pIC_{50}) illustrate an excellent relationship between experimental and predicted pIC_{50} of the training and test set compounds in CoMFA and CoMSIA, respectively (Fig. 3a, b).

The steric and electrostatic 3D contour maps (Fig. 5a, b) around the most active compound **5** explained the predicted activity of the CoMFA model. The green regions indicate areas where bulky group would favor inhibition while the yellow regions show unfavorable effects by the presence of any bulky groups. The cut-off energies for sterically favored and disfavored regions are set as 88 and 12 %, respectively. The green contours near the R_3 position indicate that bulky groups would increase the activity at this position (Fig. 5a). This finding is further supported by experimental finding that compounds **1**, **5**, **10**, **13**, and **15** possess bulkier groups at the R_3 position have higher activities compare to compounds **2**, **7**, **12**, **18**, **31**, and **53**. According to the green isopleths and docking results, no significant interactions between the ligand and surrounding residues around R_3 position are observed in Fig. 4a, b. Perhaps, it is responsible for the low activities that were

Table 3 Statistical parameters for CoMFA and CoMSIA

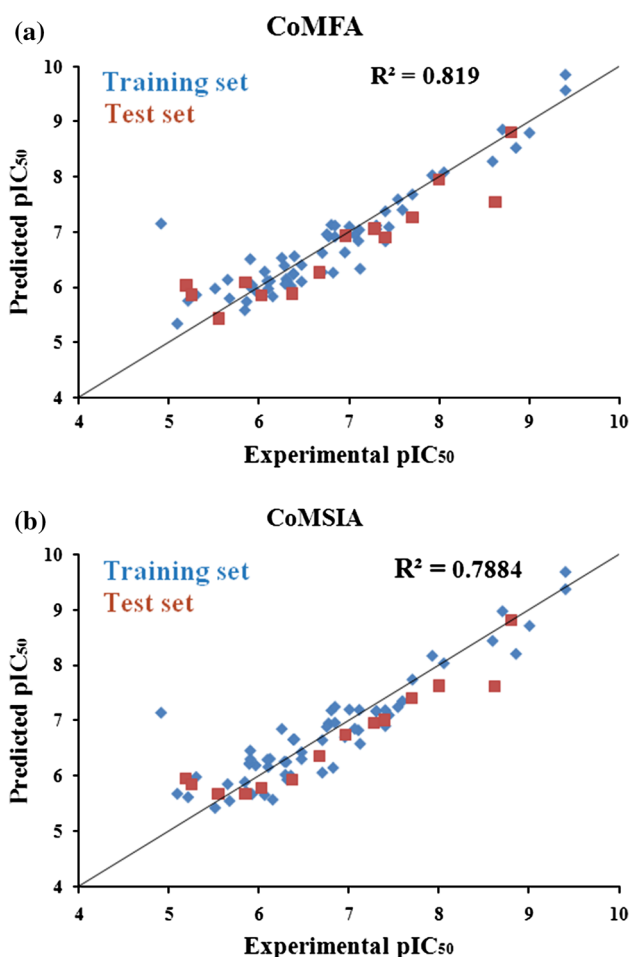
PLS statistical parameters	CoMFA	CoMSIA
q_{cv}^2 ^a	0.531	0.525
ONC ^b	5	4
r_{ncv}^2 ^c	0.913	0.889
<i>F</i> value ^d	114.879	111.970
SEE ^e	0.313	0.350
r_{pred}^2 ^f	0.77	0.79
Fraction of field contribution (%)		
Steric field	51.7 %	14.4 %
Electrostatic	48.3 %	28.0 %
Hydrophobic	—	20.5 %
Hydrogen bond acceptor	—	11.9 %
Hydrogen bond donor	—	25.2 %

^a Cross-validated correlation coefficient^b Optimum number of component^c Non-cross-validated correlation^d Fischer statistic^e standard error of estimate^f predicted correlation coefficient

observed. If a less bulky group is replaced with a bulkier steric group, the activity might be enhanced with more interactions. Some yellow contours are also present around the template. One of them is found near the R₁ position where Phe245 is also present suggesting that steric hindrance at this position could be reason for low activity. The less-hindered R₁ groups of compounds **24–27** showed higher activities while compounds **20–23** are buried near this contour due to the presence of bulkier cyclic group.

Blue and red regions indicate electron-donating or electron-attracting groups would be favored or disfavored, respectively. Positioning of different substituent at R₃ near to the blue region where electronegative Asp185 is located indicating that the activity can be enhanced by substituting electron-donating groups at this position (Fig. 5b). Compounds **1**, **9**, **13**, **43**, and **56** that contain electron-donating groups have higher activities than compounds **2**, **18**, **22**, **28**, **38**, **47**, and **53** with low electron-donating groups. A large red isopleth is located near R₂ position (Fig. 5b). Compounds **20–23** containing less electronegative nitrogen containing moieties have lower activities than compounds **24–27** which have more electronegative methoxy (OMe) substituent at the same position. The isopleths of blue and red are set at contribution levels of 85 and 15 % for encircle regions.

CoMSIA contour plots with all five descriptors are shown in Fig. 6. In CoMSIA, 80 and 20 % contribution levels were set for steric and electrostatic region, respectively. The effects of steric and electrostatic contribution in

**Fig. 3** Graphical interpretation of actual versus predicted pIC₅₀ of the training and test sets generated by the CoMFA and CoMSIA models

CoMSIA are quite similar to that found in CoMFA (Fig. 6a, b).

Hydrophilic and hydrophobic favored areas are indicated by white and yellow contours, respectively. The presence of a yellow contour near R₃ position suggested that hydrophobic substituent at this region would be responsible for better bioactivity (Fig. 6c) which is also supported by docking studies. The presence of hydrophobic Val206 and Tyr207 residues near this region also supported the action that a hydrophobic moiety at this position is favorable. Comparison of compounds **5–7**, **9**, **10**, **13**, **14**, and **19** to **2**, **17**, and **18** indicated that the cyano (CN) moiety at this region is responsible to decrease the activity. Furthermore, compounds **43**, **44**, and **48** containing a less hydrophilic R₃ group near yellow region are more active than compounds **45–47** which have more hydrophilic groups. A white isopleth near the R₂ group indicates that hydrophilic moiety would increase activity. This was evident from the observation that compounds **24–27** that have

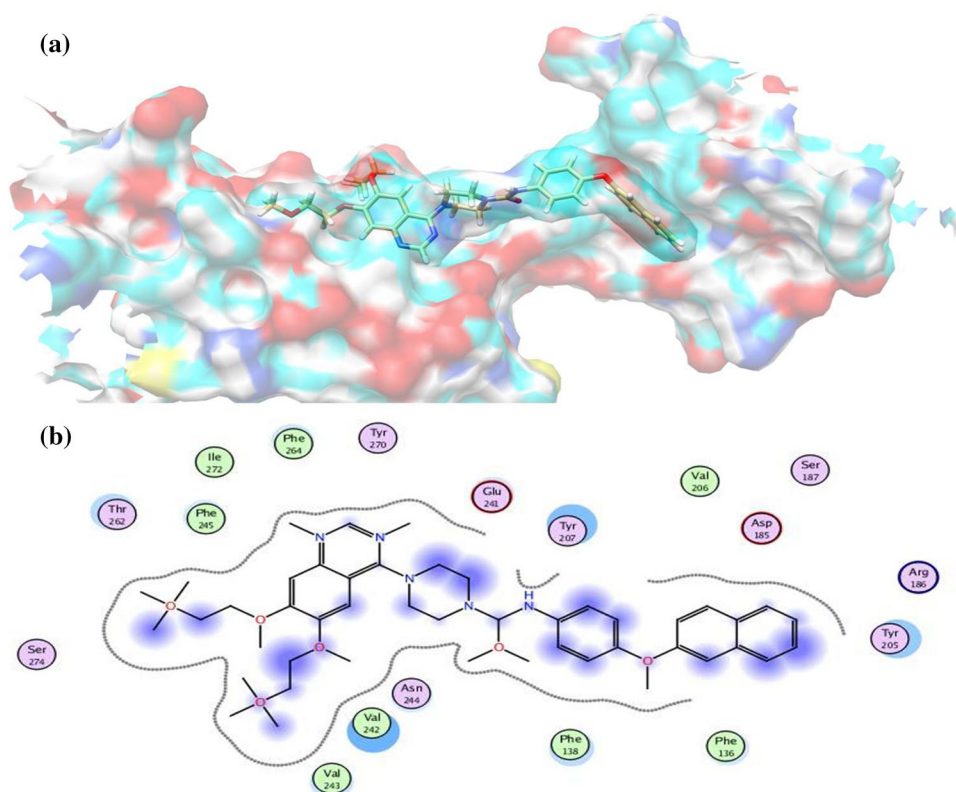


Fig. 4 **a, b** The binding conformation of active compound displayed inside binding pocket of PDGFR and 2D representation generated by MOE software of active compound **5** surrounded by binding residues of PDGFR

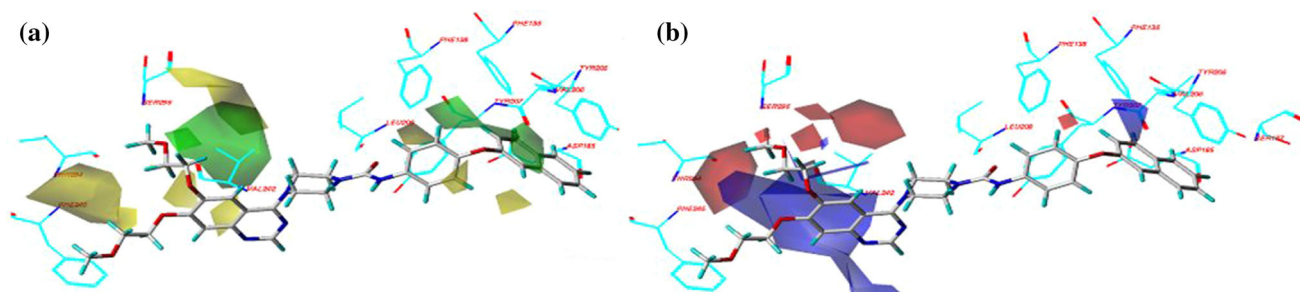


Fig. 5 Contour maps of CoMFA analysis with grid spacing in combination of compound **5**. **a** Steric field: *green* contours (favored) and *yellow* (disfavored) with 88 % contribution and 12 %

contribution, respectively. **b** Electrostatic field: *blue* contours (electropositive favored) and *red* contour (electronegative favored) (Color figure online)

nitrogen containing moieties at R_2 . Additionally, it is also evident from Fig. 6c, where R_2 group is surrounded by the Ser274 and Thr262 active site residues of PDGFR.

Hydrogen bond acceptor favorable and unfavorable fields are indicated by magenta and red contours, respectively, in Fig. 6d. Red isopleths near the R_3 group show that hydrogen bond acceptor moiety might be a reason for its low activity. At R_3 position, due to lack of hydrogen bond donor residues (Phe138, Phe136, and Tyr207) no significant interactions were observed. As a result,

compound **2** was less active than most potent compound **5**. Although, it is observed that a CN group at R_3 position in compounds **24–27** have low effects than others compounds which contain the same group. In Fig. 6e, hydrogen bond donor group is favored by cyan contour and unfavorable hydrogen bond donor groups explained by purple contour. To explain the effect of hydrogen bond donor, only single cyan contour is participating in the current study. Compounds **13** and **14** contain hydrogen bond donor moieties have higher inhibitory activity compared with compound **9**

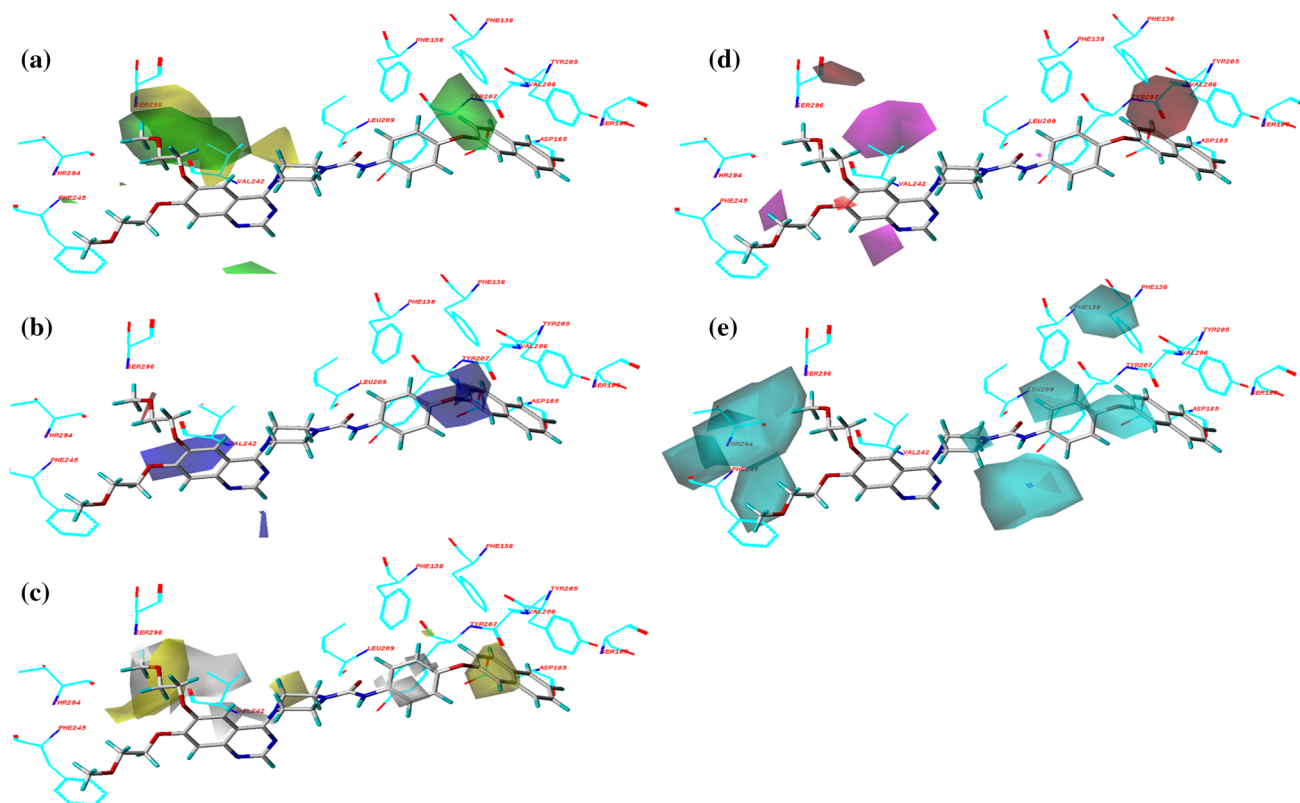


Fig. 6 Std. * coeff. contour maps of CoMSIA analysis with 2 Å grid spacing in combination with most active (compound **5**) as template. **a** Steric contour map. *Green* and *yellow* contours refer to sterically favored and disfavored regions. **b** Electrostatic contour map: *blue* and *red* contours refer to regions where electron-donating and electron withdrawing groups are favored. **c** *Yellow* contour (hydrophobic

favored) 80 % contribution and *white* contour (hydrophilic favored) 20 % contribution. **d** The CoMSIA hydrogen bond acceptor contour map in which *cyan* and *purple* (80 and 20 % contributions) contours indicated favorable and unfavorable region for hydrogen bond donor groups. **e** Hydrogen bond donor field: *cyan* contour (hydrogen bond donor favored) 80 % contribution (Color figure online)

which have a tertiary butyl (t-Bu)-substituted ring at the R₃ position. Furthermore, this effect is also demonstrated by **66** having imine group as it is located in the cyan region with a higher activity compare to **68** and **69**. The naphthalene group of compound **5** is surrounded by Phe136, Tyr207, and Val206. The benzyl ring of Phe138 forms strong hydrophobic interactions with the benzene ring of active compounds. Furthermore, Phe206 interacts with 1,2-dimethoxyethane near the quinazoline ring indicating hydrophobicity that would be favorable to enhance the activity.

Conclusion

In conclusion, CoMFA and CoMSIA studies provided valuable understanding about the structural features affecting the activity of PDGFR inhibitors. The docking results along with contour maps well-explained structural features influencing on the inhibitory activity. CoMFA- and CoMSIA-generated 3D-QSAR models showed good q^2 and r^2 values and revealed a beneficial response in test set

validation. These models provide the tool for guiding the design and synthesis of novel and more potent PDGFR derivatives.

Acknowledgments Authors are highly acknowledged Higher Education Commission (HEC) of Pakistan for their financial support, and also grateful to Prof. Bernd M. Rode (University of Innsbruck) for providing their technical and software support to conduct this research work.

References

- Clark M, Cramer RD, Van Opdenbosch N (1989) Validation of the general purpose Tripos 5.2 force field. *J Comput Chem* 10(8):982–1012
- Cramer RD, Patterson DE, Bunce JD (1988) Comparative molecular field analysis (CoMFA). 1. Effect of shape on binding of steroids to carrier proteins. *J Am Chem Soc* 110(18):5959–5967
- Du-Cuny L, Song Z, Moses S, Powis G, Mash EA, Meuillet EJ, Zhang S (2009) Computational modeling of novel inhibitors targeting the AKT pleckstrin homology domain. *Bioorg Med Chem* 17(19):6983–6992
- Gasteiger J, Marsili M (1980) Iterative partial equalization of orbital electronegativity—a rapid access to atomic charges. *Tetrahedron* 36(22):3219–3228

- Geladi P, Xie YL, Polissar A, Hopke P (1998) Regression on parameters from three-way decomposition. *J Chemom* 12(5):337–354
- Geldenhuis WJ, Nakamura H (2010) 3D-QSAR and docking studies on transforming growth factor (TGF)-beta receptor 1 antagonists. *Bioorg Med Chem Lett* 20(6):1918–1923
- Guha R, Jurs PC (2004) Development of linear, ensemble, and nonlinear models for the prediction and interpretation of the biological activity of a set of PDGFR inhibitors. *J Chem Inf Comput Sci* 44(6):2179–2189
- Gupta P, Roy N, Garg P (2009) Docking-based 3D-QSAR study of HIV-1 integrase inhibitors. *Eur J Med Chem* 44(11):4276–4287
- Klebe G, Abraham U, Mietzner T (1994) Molecular similarity indices in a comparative analysis (CoMSIA) of drug molecules to correlate and predict their biological activity. *J Med Chem* 37(24):4130–4146
- Kurup A, Garg R, Hansch C (2001) Comparative QSAR study of tyrosine kinase inhibitors. *Chem Rev* 101(8):2573–2600
- Pandey A, Volkots DL, Seroogy JM, Rose JW, Yu J-C, Lambing JL, Hutchaleelaha A, Hollenbach SJ, Abe K, Giese NA (2002) Identification of orally active, potent, and selective 4-piperazinylquinazolines as antagonists of the platelet-derived growth factor receptor tyrosine kinase family. *J Med Chem* 45(17):3772–3793
- Qin J, Lei B, Xi L, Liu H, Yao X (2010) Molecular modeling studies of Rho kinase inhibitors using molecular docking and 3D-QSAR analysis. *Eur J Med Chem* 45(7):2768–2776
- Roques BP, Noble F, Dauge V, Fournie-Zaluski MC, Beaumont A (1993) Neutral endopeptidase 24.11: structure, inhibition, and experimental and clinical pharmacology. *Pharmacol Rev* 45(1):87–146
- Sethi KK, Verma SM, Prasanthi N, Sahoo SK, Parhi RN, Suresh P (2010) 3D-QSAR study of benzene sulfonamide analogs as carbonic anhydrase II inhibitors. *Bioorg Med Chem Lett* 20(10):3089–3093
- Seymour AA, Swerdel JN, Abboa-Offei B (1991) Antihypertensive activity during inhibition of neutral endopeptidase and angiotensin converting enzyme. *J Cardiovasc Pharmacol* 17(3):456–465
- Shim AH-R, Liu H, Focia PJ, Chen X, Lin PC, He X (2010) Structures of a platelet-derived growth factor/propeptide complex and a platelet-derived growth factor/receptor complex. *Proc Natl Acad Sci* 107(25):11307–11312
- SYBYL 7.3; Tripos Inc.: 1699 South Hanley Rd., St. Louis, MO 63144
- Ul-Haq Z, Mahmood U, Jehangir B (2009) Ligand-based 3D-QSAR studies of physostigmine analogues as acetylcholinesterase inhibitors. *Chem Biol Drug Des* 74(6):571–581
- Zhang N, Zhong R (2010) Docking and 3D-QSAR studies of 7-hydroxycoumarin derivatives as CK2 inhibitors. *Eur J Med Chem* 45(1):292–297
- Zhong C, He J, Xue C, Li Y (2004) A QSAR study on inhibitory activities of 1-phenylbenzimidazoles against the platelet-derived growth factor receptor. *Bioorg Med Chem* 12(15):4009–4015